ACS Macro Letters

Letter

pubs.acs.org/macroletters

# Kinetic Polymer Arrest in Percolated SWNT Networks

Rana Ashkar,*[,†,‡] Mansour Abdul Baki,[§] Madhusudan Tyagi,[†,‡] Antonio Faraone,[†,‡] Paul Butler,*[,‡,∥] and Ramanan Krishnamoorti*[,§]

[†]Materials Science and Engineering Department, University of Maryland, College Park, Maryland 20742, United States

[‡]National Institute of Standards and Technology, Gaithersburg, Maryland 20899, United States

[§]Department of Chemical & Biomolecular Engineering, University of Houston, Houston, Texas 77204, United States

[∥]Department of Chemical Engineering, University of Delaware, Newark, Delaware 19711, United States

Supporting Information

**ABSTRACT:** Particle−polymer attractions in nanocomposites can cause significant heterogeneities in the polymer dynamics and remarkably impact the material properties. Dynamical perturbations are generally expected to be limited to interfacial polymer segments. However, composites with highly anisotropic nanoparticles usually exhibit very low percolation thresholds. In such systems, the overlapping interfacial regions could result in a complex polymer relaxation behavior that is unanticipated from dilute nanoparticle dispersions in polymer matrices. To understand this behavior, we examine a system of percolated single-wall carbon nanotubes (SWNT) in a polymer matrix, PMMA, which is known to have strong interfacial binding. Neutron spectroscopy measurements on the composites reveal not only an interfacial polymer layer that is transiently pinned to the SWNT surface, but suggest that the percolated network forms a kinetic cage that dramatically restricts both local and cooperative relaxations of noninterfacial polymer segments. These findings should help guide theories and simulations of hierarchical polymer dynamics in nanocomposites.

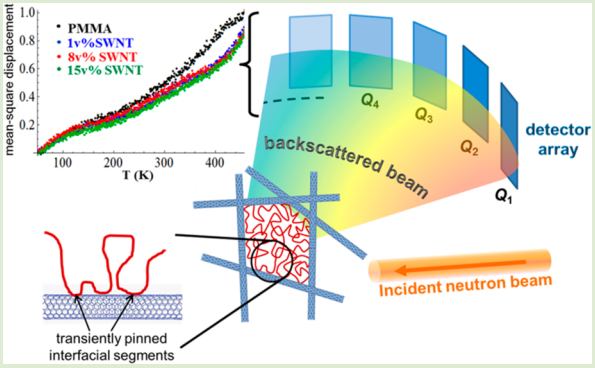


Single-wall carbon nanotube (SWNT) polymer composites have gained significant attention as candidates for a number of advanced applications owing to the unique mechanical, optical, and conductive properties of SWNTs.[1,2] The superior performance of these composites is believed to emerge from the synergistic integration of the nanotube properties with those of the polymer.[3] Indeed, dispersing nanoparticles in a polymer matrix usually modifies the static and dynamic properties of the matrix, leading to substantial deviations from the pure polymer behavior[4−6] and sometimes resulting in rather unexpected properties.[7] However, despite a fairly large body of work,[8−10] a good understanding of how the inclusion of nanoparticles perturbs the static and dynamic properties of the polymer remains unresolved.

While many studies have focused on the performance of SWNT composites,[11−13] very few address polymer dynamics[14,15] in these systems, despite the recent recognition that they are intimately linked with their structural features and are fundamental to the design of material properties such as plasticity,[16] fragility,[17] gas permeation,[18] and physical aging.[7,19] Moreover, research on dynamics tends to focus on nanocomposites with spherical particles and extrapolation to composites with rod-like SWNTs and plate-like clays and graphene is nontrivial. The challenge is partly due to the highly anisotropic nature of such nanoparticles which, combined with their impenetrability and rigidity, can alter the polymer properties in unconventional ways[20] that cannot be captured with classical nanocomposite theories.[8] In the absence of adequate theories, molecular dynamic simulations have been used to provide insight into the microscopic dynamics in this unique type of composite. For carbon nanotube composites in particular, a recent molecular dynamic (MD) simulation,[15] performed with a single nanotube, showed that even in this simple case of isolated SWNTs the dynamics are quite complex and are strongly affected by interfacial interactions. In the case of favorable polymer/nanotube interactions, the simulation reports remarkable dynamic heterogeneities between bulk polymer chains and chains that are in contact with the nanotube; the latter experience significant suppression in their mean-square displacements (MSD) at otherwise comparable conditions. Furthermore, the simulated composite is shown to have slow polymer domains in the vicinity of the SWNT and faster bulk domains away from the nanotube surface, a phenomenon that has been observed in simulations of other nanocomposites.[21,22] In the case of a percolated nanotube network, the slow domains around the nanotubes start to

**Received:** October 4, 2014
**Accepted:** November 25, 2014
**Published:** December 3, 2014

  

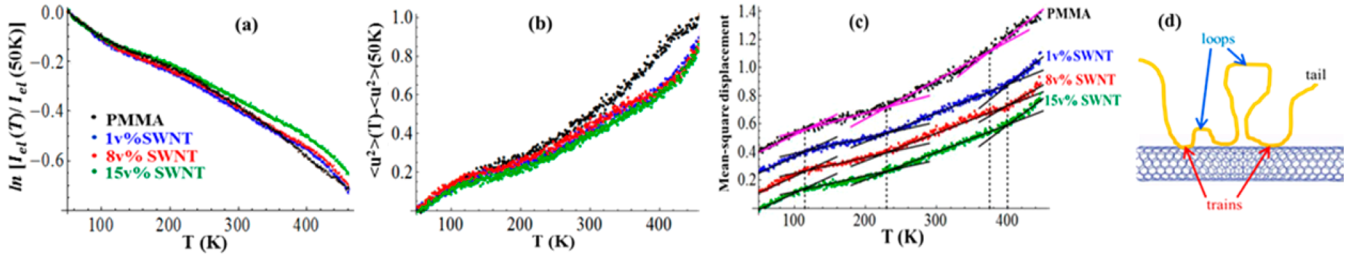


**Figure 1.** (a) Incoherent elastic scattering intensity from PMMA and the PMMA composites with various SWNT loadings summed over all detectors for 50 K < $T$ < 460 K. (b) MSD amplitude in the pure polymer and in the SWNT composites showing shorter-range atomic motions in the composites. (c) Identification of the dynamic phases in PMMA and the composite showing the crossover temperatures (dotted lines) associated with the onset of motions described in the text; the data sets are shifted vertically for clarity. Error bars represent ±1 standard deviation in all the plots. In the figures above, the error bars are smaller than the plot symbols. (d) Schematic representation of the polymer configuration in terms of train, loop, and tail segments.

overlap, rendering the overall polymer dynamics more complicated. Unfortunately, available MD models have not been extended to systems with nanotube networks and cannot capture the associated dynamical complexities.

Direct experimentation is then needed to understand the effects of nanotube percolation on the dynamics of the polymer matrix. The challenge in experimental studies on such systems is the difficulty in directly accessing the length and time scales of interest. In this regard, neutron spectroscopy techniques offer unique means for probing selective dynamics in polymer composites. The advantage of such techniques over other experimental approaches lies in the capability of resolving dynamical processes over length and time scales[23,24] that are compatible with atomistic motions and segmental relaxations in polymeric systems. In particular, neutron backscattering and neutron spin−echo (NSE) spectroscopy are frequently utilized for probing local atomic motions and chain relaxations in polymer systems.

Backscattering elastic window scans were performed on poly(methyl methacrylate) (PMMA) and PMMA composites with 1, 8, and 15% volume fraction SWNTs over a wide range of temperatures, $T$. This type of measurement yields the elastic incoherent scattering intensity, $I_{el}^{inc}(Q)$, as a function of accessible wavevector transfer $Q$. Integrating the intensity over the entire $Q$ range of the measurement leads to the $T$-dependent $I_{el}^{inc}$ shown in Figure 1a, where the intensity at each temperature is normalized to the intensity at $T$ = 50 K for that sample. Within the energy resolution of the HFBS spectrometer[25] (≈ 1 $\mu$ev), all motions slower than ≈2 ns appear static and thus will be recorded as elastic scattering events. However, motions faster than this time frame contribute to nonelastic scattering and lower the intensity of the elastic signal. This effect is clearly seen in Figure 1a where the elastic intensity decreases with increasing temperature as the mobility of the polymer increases.

On the other hand, it is clear that the decrease in elastic intensity with temperature is not as rapid for the SWNT composites as for the pure PMMA at high temperatures, indicating that the inclusion of nanotubes has reduced the fraction of hydrogen atoms whose motion is faster than 2 ns. While this could be interpreted as a general decrease in polymer mobility by a uniform slowing down of the spectrum of motions, it would also be consistent with simulations on nanocomposites with attractive polymer−particle interactions[22] and a previous report on PMMA-C60 composites,[26] which suggest that the interfacial polymer segments are transiently pinned for times longer than the 2 ns window of our measurement. In the language of polymer adsorption, the polymer chain can be described as sequences of train segments, in contact with the nanotubes, and loop and tail segments away from the interface (Figure 1d). In this scenario, while the mobility of loop and end segments could be affected, the measured decrease in mobility would come primarily from an increasing amount of pinned train segments now contributing to the apparently elastic signal as the amount of SWNTs is increased.

By analyzing the $Q$-dependence of $I_{el}^{inc}(Q)$ rather than integrating over all $Q$, we can extract the spatial range of the atomic motions (Figure 1b). A clear contraction in the mean-square displacement, $\langle u^2 \rangle$, is observed in the composites compared to pure PMMA, but the MSDs in the different composites are largely unaffected by the SWNT loading. Assuming a model of transiently pinned train segments, this invariance with SWNT loading would suggest that, despite the decreasing fraction of loops and ends, the extent of mobility of the remaining "free" segments is unchanged.

In order to better understand the potential effects of any pinned interfacial layers, some discussion of the state of dispersion in these SWNT networks is required. In ideal dispersions, increasing SWNT loading generates a tighter network with smaller mesh size, but previous studies on systems with comparable loadings show that the dispersions at such concentrations are far from ideal. However, even in such nonideal dispersions comprising micron-size flocs of SWNT networks,[27,28] the networks tend to get more compact with increasing nanotube concentration. A rough estimate of the mesh size of the SWNT network in the current composites is calculated[29] for dispersions of nanotube bundles of ∼8 nm diameter (as observed from TEM images in the Supporting Information) to be 7−28 nm for the range of concentrations considered here and is in agreement with SANS results on similar systems.[27,30] For the composite with a SWNT volume fraction of 15%, the mesh size (7 nm) is smaller than the average unperturbed coil dimension ($2R_g \approx 29$ nm, with $R_g$ being the radius of gyration of the polymer), but is on the same order as $2R_g$ for the composite with 1% loading. Thus, at higher loadings, a given polymer chain is expected to make more contacts with the SWNT network so that even the non-interfacial polymer units might be expected to be more constrained. However, the data show that the atomic displacements are hardly affected by the compactness of the SWNT network which implies that the localized hydrogen motions are constrained by the percolated SWNT network, but not further affected by the proximity of the interface. Combined


dx.doi.org/10.1021/mz500636s | ACS Macro Lett. 2014, 3, 1262−1265

with the fact that the total hydrogen mobility decreases with increasing SWNT loading, this begins to suggest the possible coexistence of two distinct polymer regions in the presence of the nanotubes: regions with effectively frozen dynamics around the nanotubes and regions with faster motions away from the interface. The resultant scheme is one in which the slow interfacial segments arrest the faster noninterfacial segments and restrict the extent of their local mobility. This observation is reminiscent of dynamic heterogeneity in dynamically asymmetric miscible polymer blends in which the dynamics of the fast component are found to be effectively restricted by the slower one.[31−33]

More insight about the energetics driving these local motions can be inferred from the thermal dependence of the MSD patterns. Within the harmonic model, the $T$-dependence of $\langle u^2 \rangle$ is given by $\langle u^2 \rangle = 3k_BT/\kappa$, where $\kappa$ is the effective material stiffness and $k_B$ is the Boltzmann constant. This is based on the assumption that the internal energy of the system is purely vibrational and applying it outside the low-$T$ vibration regime is heuristic. However, it is fair to assume that thermally induced motions increase the degrees of freedom in the system and result in a change of the numerical coefficient in the previous expression while maintaining a linear $T$-dependence of the MSDs.

This approach provides a qualitative framework for identifying different dynamic phases in the MSD patterns over the explored temperature range (Figure 1c). The crossover temperatures, at which a change in the slope is observed, designate a transition in the local dynamics and are found to occur at $T$ = 120 and 230 K for all samples and at $T$ = 380 and 400 K for PMMA and the composites, respectively. The two lowest transitions signify the onset of classical hopping of the ester-methyl group (≈ 120 K)[34] and the activation of the rotational $\alpha$-methyl group (≈ 230 K).[35] The highest-$T$ crossover is associated with segmental relaxations and denotes the glass transition temperature, $T_g$. For PMMA, $T_g$ is found to be ≈ 380 K, in agreement with literature values.[36] The compo sites, on the other hand, exhibit an increase of ≈ 20 K in $T_g$. Such increases in $T_g$ have been observed in composites with strong attractive polymer/particle potentials, but the shift that we observe in the present samples is higher than what has been generally reported on unfunctionalized nanotube composites.[9] In a theoretical study, Long and Lequeux[37] postulated that the shift in the glass transition to higher temperatures is driven by the connectedness of slow domains throughout the system requiring higher thermal energy to collectively overcome the kinetic barrier of the glassy state. In analogy, the noticeable increase in $T_g$ that we observe is another indication in favor of the scheme of percolated slow polymer regions and is consistent with the picture of dynamically arrested train segments around the percolated SWNTs.

The $T_g$ shifts obtained in the MSD data qualitatively suggest a slowdown in the structural relaxations in the composites but cannot provide a quantitative description of those relaxations as they mostly lie outside the time window of the elastic scans. It is also important to recognize that segmental relaxations are collective motions that are determined by the cooperativity of the polymer segments. For this, we use coherent neutron spin−echo (NSE) spectroscopy which primarily detects relaxations of collective dynamics in the probed sample. In order to obtain a strong correlated signal and to minimize the contribution of incoherent scattering from hydrogen atoms, NSE measurements were carried out using deuterated PMMA (dPMMA) and a dPMMA composite with 8% loading. The NSE instrument was tuned to selectively probe dynamics at $Q$ = 0.9 Å$^{-1}$, at which the chain−chain relaxations are expected to be most prominent (see Supporting Information). NSE measurements yield the intermediate scattering function $S(Q, t)$ which, for polymers, is described by a stretched exponential of the Kohlrausch−Williams−Watts form: $S(Q, t)/S(Q, 0)$ = DWF × $\exp[-(t/\tau_R)^{\beta}]$, where $\tau_R$ is the temperature-dependent relaxation time and $\beta$ is the stretching exponent that defines the distribution of the decay modes. The $\beta$-values are found to be 0.71 for dPMMA and 0.52 for the composite and are consistent with the picture of increased dynamical heterogeneities in the composite (see Supporting Information). The values of $\tau_R$, obtained from the KWW-fits, exhibit an exponential behavior (Figure 2), which can be captured by an

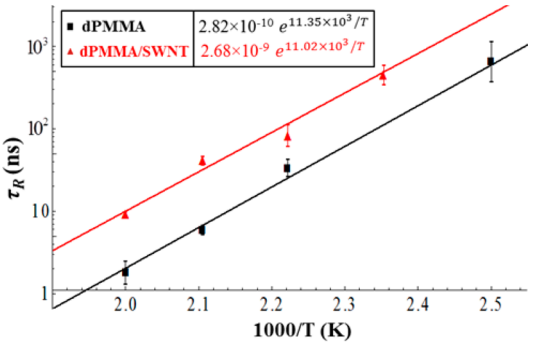


**Figure 2.** T-dependence of the segmental relaxation times in dPMMA and the SWNT/dPMMA composite with 8% loading, as extracted from NSE data. The relaxations in the composite are approximately an order of magnitude slower than in dPMMA.

Arrhenius function $\tau_R = \tau_0 \exp[E_A/k_BT]$, where $\tau_0$ is a pre-exponential factor and $E_A$ is the activation energy. The Arrhenius fits indicate that the pure polymer and the SWNT composite experience similar trends in the relaxation process, manifested in almost identical activation energies, $E_A \approx 38.5k_BT$. The similarity of the activation energy in nanocomposites with that of the unfilled polymer has been reported in a number of recent studies[38] and implies that the inclusion of the nanotubes does not disrupt the energy barrier required for structural relaxations of the host polymer. The other striking feature in Figure 2 is that the relaxations, set by $\tau_0$, are an order of magnitude slower in the composite than they are in the pure polymer. Drawing from collision theory, this is analogous to a lower frequency factor, which can be interpreted as a decrease in the number of polymer segments that can collectively relax at a given temperature. Combined with the earlier backscattering interpretation, these findings suggest that the local pinning of train segments results in a dramatic slowdown of the structural relaxations in the composite due to the connectivity of the polymer chains.

Taken as a whole, our results strongly support a picture of two dynamic populations with the interfacial train segments experiencing a transient immobilization, while the remaining loop and end segments remain mobile. In a percolated SWNT network, the immobile segments exert a dynamic cage for the polymers within the percolated mesh, which results in a restriction in the local modes of the loop segments and a subsequent slowdown in the longer-range relaxations. It is interesting to note that all of these effects are at some level driven by the surface interactions and thus presumably by the


dx.doi.org/10.1021/mz500636s | ACS Macro Lett. 2014, 3, 1262−1265

available particle surface area. One of the signature features of nanoparticles is their very high surface to volume ratio causing surface effects to dominate the physics of these systems. The use of one-dimensional nanotubes exacerbates that effect in that thin one-dimensional object yield the maximum surface to volume ratio for a given particle volume. In this framework, it would be interesting to explore the same dynamics in a system of spherical particles (with a minimum surface to volume ratio for a given particle volume) as a function of both total surface area and total volume fraction. This could help untangle surface area effects from topological and concentration effects. Another interesting case is to explore the effect of a percolated network with mesh sizes much larger than the polymer $R_g$ to study to what extent caging might trap truly free polymers.

## ■ ASSOCIATED CONTENT

### Supporting Information

Experimental details, model fitting, and supplementary experimental evidence. This material is available free of charge via the Internet at http://pubs.acs.org.

## ■ AUTHOR INFORMATION


### Corresponding Authors

*E-mail: rana.ashkar@nist.gov.
*E-mail: butler@nist.gov.
*E-mail: ramanan@uh.edu.


### Notes

The authors declare no competing financial interest.

## ■ ACKNOWLEDGMENTS

M.A.B. and R.K. gratefully acknowledge the support of the Texas Institute for Intelligent Bio-Nano Materials and Structures for Aerospace Vehicles, funded by NASA Cooperative Agreement #NCC-1-02038, and the National Science Foundation (CMMI-0708096). This work utilized the NIST Center for Neutron Research (NCNR) supported in part by the National Science Foundation under Grant #DMR-0944772. The authors thank Dr. Michihiro Nagao for experimental assistance with NSE measurements and Dr. Bharath Natarajan for his help with TEM imaging.

## ■ REFERENCES


(1) Coleman, J. N.; Khan, U.; Gun'ko, Y. K. *Adv. Mater.* **2006**, *18*, 689.
(2) Moniruzzaman, M.; Winey, K. I. *Macromolecules* **2006**, *39*, 5194.
(3) Kumar, S. K.; Krishnamoorti, R. *Annu. Rev. Chem. Biomol. Eng.* **2010**, *1*, 37.
(4) Levi, N.; Czerw, R.; Xing, S.; Iyer, P.; Carroll, D. L. *Nano Lett.* **2004**, *4*, 1267.
(5) Priya, L.; Jog, J. P. *J. Polym. Sci., Part B: Polym. Phys.* **2002**, *40*, 1682.
(6) Abdul Baki, M. *Doctoral Thesis*, University of Houston, Houston, TX, 2011.
(7) Putz, K. W.; Mitchell, C. A.; Krishnamoorti, R.; Green, P. F. *J. Polym. Sci., Part B: Polym. Phys.* **2004**, *42*, 2286.
(8) Bhattacharya, S.; Gupta, R.; Kamal, M. *Polymeric Nanocomposites Theory and Practice*; Hanser: Munich, Berlin, 2007.
(9) Grady, B. P. *J. Polym. Sci., Part B: Polym. Phys.* **2012**, *50*, 591.
(10) Sternstein, S. S.; Zhu, A.-J. *Macromolecules* **2002**, *35*, 7262.
(11) Du, F.; Fischer, J. E.; Winey, K. I. *Phys. Rev. B* **2005**, *72*, 121404.
(12) Chatterjee, T.; Krishnamoorti, R. *Soft Matter* **2013**, *9*, 9515.
(13) Kashiwagi, T.; Fagan, J.; Douglas, J. F.; Yamamoto, K.; Heckert, A. N.; Leigh, S. D.; Obrzut, J.; Du, F.; Lin-Gibson, S.; Mu, M. *Polymer* **2007**, *48*, 4855.
(14) Mu, M.; Clarke, N.; Composto, R. J.; Winey, K. I. *Macromolecules* **2009**, *42*, 7091.
(15) Karatrantos, A.; Composto, R. J.; Winey, K. I.; Kröger, M.; Clarke, N. *Macromolecules* **2012**, *45*, 7274.
(16) Riggleman, R. A.; Douglas, J. F.; de Pablo, J. J. *Soft Matter* **2010**, *6*, 292.
(17) Oh, H.; Green, P. F. *Nat. Mater.* **2009**, *8*, 139.
(18) Sharma, A.; Kumar, S.; Tripathi, B.; Singh, M.; Vijay, Y. *Int. J. Hydrogen Energy* **2009**, *34*, 3977.
(19) Green, P.; Oh, H.; Akcora, P.; Kumar, S. In *Dynamics of Soft Matter*; García Sakai, V., Alba-Simionesco, C., Chen, S.-H., Eds.; Springer: New York, 2012; p 349.
(20) Yamamoto, U.; Schweizer, K. S. *ACS Macro Lett.* **2013**, *2*, 955.
(21) Starr, F. W.; Schrøder, T. B.; Glotzer, S. C. *Macromolecules* **2002**, *35*, 4481.
(22) Desai, T.; Keblinski, P.; Kumar, S. K. *J. Chem. Phys.* **2005**, *122*, 134910.
(23) Arbe, A.; Alvarez, F.; Colmenero, J. *Soft Matter* **2012**, *8*, 8257.
(24) Colmenero, J.; Arbe, A. *J. Polym. Sci., Part B: Polym. Phys.* **2013**, *51*, 87.
(25) Meyer, A.; Dimeo, R. M.; Gehring, P. M.; Neumann, D. A. *Rev. Sci. Instrum.* **2003**, *74*, 2759.
(26) Kropka, J. M.; Garcia Sakai, V.; Green, P. F. *Nano Lett.* **2008**, *8*, 1061.
(27) Chatterjee, T.; Jackson, A.; Krishnamoorti, R. *J. Am. Chem. Soc.* **2008**, *130*, 6934.
(28) Hobbie, E. K.; Fry, D. J. *J. Chem. Phys.* 2007, *126*.
(29) Ogston, A. G. *Trans. Faraday Soc.* **1958**, *54*, 1754.
(30) Tung, W.-S.; Bird, V.; Composto, R. J.; Clarke, N.; Winey, K. I. *Macromolecules* **2013**, *46*, 5345.
(31) Tyagi, M.; Arbe, A.; Colmenero, J.; Frick, B.; Stewart, J. R. *Macromolecules* **2006**, *39*, 3007.
(32) Götze, W.; Sperl, M. *Phys. Rev. E* **2002**, *66*, 011405.
(33) Genix, A. C.; Arbe, A.; Alvarez, F.; Colmenero, J.; Willner, L.; Richter, D. *Phys. Rev. E* **2005**, *72*, 031808.
(34) Moreno, A. J.; Alegría, A.; Colmenero, J.; Frick, B. *Macromolecules* **2001**, *34*, 4886.
(35) Colmenero, J.; Moreno, A. J.; Alegría, A. *Prog. Polym. Sci.* **2005**, *30*, 1147.
(36) Colby, R. H. *Phys. Rev. E* **2000**, *61*, 1783.
(37) Long, D.; Lequeux, F. *Eur. Phys. J. E* **2001**, *4*, 371.
(38) Vingaard, M.; de Claville Christiansen, J. *J. Mater. Sci.* **2011**, *46*, 4660.